

Diameter selective characterization of single-wall carbon nanotubes

F. Simon, Á. Kukovecz*, C. Kramberger, R. Pfeiffer, F. Hasi, and H. Kuzmany
Institut für Materialphysik, Universität Wien, Strudlhofgasse 4, A-1090 Wien, Austria

H. Kataura
Department of Physics, Tokyo Metropolitan Univ, Tokyo, Japan

A novel method is presented which allows the characterization of diameter selective phenomena in SWCNTs. It is based on the transformation of fullerene peapod materials into double-wall carbon nanotubes and studying the diameter distribution of the latter. The method is demonstrated for the diameter selective healing of nanotube defects and yield from C₇₀ peapod samples. Openings on small diameter nanotubes are closed first. The yield of very small diameter inner nanotubes from C₇₀ peapods is demonstrated. This challenges the theoretical models of inner nanotube formation. An anomalous absence of mid-diameter inner tubes is observed and explained by the suppressed amount of C₇₀ peapods due to the competition of the two almost equally stable standing and lying C₇₀ peapod configurations.

Nanostructures based on carbon nanotubes [1] have been in the forefront of nanomaterial research in the last decade. However, there still remains a number of open questions before one of the most promising candidates, single-wall carbon nanotubes (SWCNTs) will have wide-spread applications. The most important obstacle is the large number of electronically different nanotubes produced with similar diameters and different chiralities [2]. To overcome this, recent efforts have focused on separation of SWCNTs [3][4][5][6]. The general problem remaining before the successful optimization of such methods is the identification of the separated SWCNTs according to their chiral vectors. Another prerequisite for the applicability of SWCNTs is the capability of studying the behavior of different SWCNTs against chemical and physical treatments in a chirality sensitive manner. Band-gap fluorescence was successfully applied to assign the chiral index to semiconducting SWCNTs [7]. In a different approach, assignment to chiral vectors of small diameter nanotubes in double-wall carbon nanotubes (DWCNTs) was performed using Raman spectroscopy [8][9]. DWCNTs are SWCNTs containing a coaxial, smaller diameter CNT. The material is produced from fullerene encapsulated SWCNT materials, known as peapods [10], by a high temperature treatment [11].

The above mentioned chirality assignment method by Raman spectroscopy is at first glance not automatically applicable for studying the properties of the outer tubes and, in addition, seemingly suffers from several limitations such as e.g. openings on the outer tubes are required. In addition, the growth process of DWCNTs from fullerene peapods is not yet understood. From computer simulation, it was demonstrated that C₆₀@SWCNT, peapod, based DWCNTs are formed by Stone-Wales transformations from C₆₀ dimer precursors formed at high temperature by cyclo-addition [12][13]. The free rotation of C₆₀ molecules is a prerequisite for the dimer formation as it enables the molecules to have facing double bonds. It has been found experimentally that the ellip-

soidal shaped C₇₀ are present as both standing or lying peapod configurations i.e. with the longer C₇₀ axis perpendicular or parallel to the tube axis [14][15].

In this Letter, we show that assigning the chiralities of the inner nanotubes of DWCNT samples is a useful tool as the inner nanotube distribution mimics that of the outer tubes. This allows the characterization of diameter selective reactions or the measurement of the nanotube abundance in the starting material. This is demonstrated on the diameter selective healing of the SWCNT openings. Furthermore, the comparison of C₆₀@SWCNT and C₇₀@SWCNT based DWCNTs evidences that the distribution of inner tubes is very similar in the two kinds of samples. A dramatic exception is observed for the $d \approx 0.67$ nm inner nanotubes for which the corresponding outer tubes are on the border between lying and standing C₇₀ configurations. Such inner tubes are nearly absent in the C₇₀@SWCNT based DWCNTs. The presence of very small inner nanotubes, that can only be based on lying C₇₀, challenges the current theoretical models of inner tube formation.

We prepared C₆₀,C₇₀@SWCNT based DWCNTs (60-DWCNT and 70-DWCNT, respectively) from different SWCNT materials. Two arc-discharge prepared commercial SWCNTs (SWCNT-N1 and N2 from Nanocarblab, Moscow, Russia [16]) and laser ablation prepared commercial (SWCNT-R from Tubes@Rice, Houston, USA) and laboratory prepared SWCNT (SWCNT-L) were used. The SWCNT-L samples are identical to those used previously [8][9]. The SWCNT-N1, N2 materials were purified to 50 % with repeated high temperature air and acid washing treatments by the manufacturer. SWCNT-R and SWCNT-L materials were purified following Ref. [17]. Peapod samples were prepared by annealing SWCNT with C₆₀ in a quartz tube following Ref. [17] and were transformed to DWCNT at high temperature following Ref. [11]. The diameter distributions of the SWCNT materials were determined from Raman spectroscopy [18] giving $d_{N1} = 1.50$ nm, $\sigma_{N1} = 0.10$ nm,

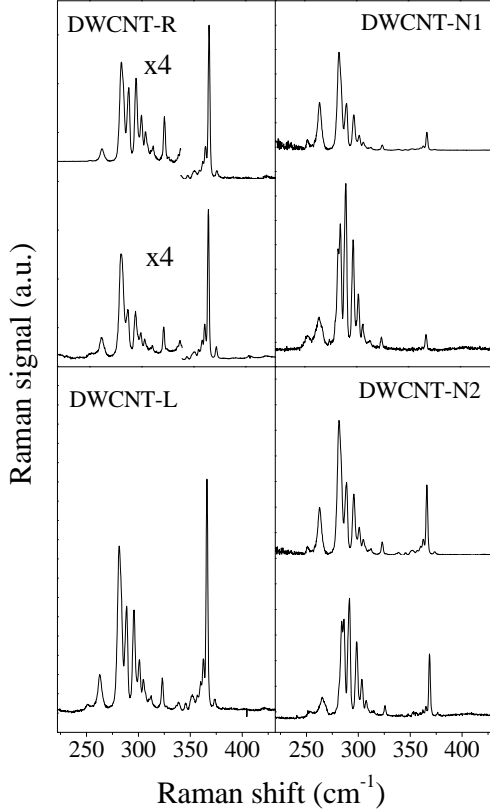


FIG. 1: As measured Raman spectra of the inner nanotube RBMs for four 60-DWCNT samples (lower curves) at 647 nm laser excitation. The upper spectra are smart scaled from the lower left spectrum (DWCNT-L). The agreement between the as measured and smart scaled spectra are obvious even though e.g. the N1, N2 tubes have clearly different diameters.

$d_{N2} = 1.45$ nm, $\sigma_{N1} = 0.10$ nm, $d_R = 1.35$ nm, $\sigma_R = 0.09$ nm, and $d_L = 1.39$ nm, $\sigma_L = 0.09$ nm for the mean diameter and the variance of the distribution for the different samples, respectively. We have verified that the results described here are reproducible for all the samples. Multi frequency Raman spectroscopy was performed on a Dilor xy triple axis spectrometer in the 1.64-2.54 eV (755-488 nm) energy range and in a Bruker FT-Raman spectrometer for the 1.16 eV (1064 nm) excitation at 90 K. The spectral resolution was 1-2 cm^{-1} depending on the laser wavelength. Raman shifts were calibrated against a series of spectral calibration lamps.

In Fig. 1., we compare Raman spectra of the different 60-DWCNT materials for a 647 nm excitation. The spectra are representative for the overall picture observed for the measurements at other exciting laser energies and represent the response from the radial breathing mode (RBM) of inner tubes only. The splitting of the RBMs of geometrically allowed tubes is also observed in Fig. 1. It was suggested to originate from one type of inner tubes being encapsulated in outer tubes with slightly different tube diameters [8]. Interestingly, the RBMs of all the

observable inner tubes, including the split components, can be found at the same position in all DWCNT samples within the $\pm 0.5 \text{ cm}^{-1}$ experimental precision of our measurement for the whole laser energy range studied here. This agreement between the different samples proves that vibrational modes of DWCNT samples are robust against the starting material. This robustness goes beyond the pure mode frequencies.

As the four samples have different diameter distributions, the overall Raman patterns look different. However, scaling the patterns with the ratio of the distribution functions allows to generate the overall pattern for all systems, starting from e.g. DWCNT-L in the bottom-left corner of Fig.1. It was assumed that the inner tube diameter distributions follow a Gaussian function with a mean diameter 0.72 nm smaller than those of the outer tubes based on a previous determination [19] and with the same variance as the outer tubes. We used the empirical constants from Ref. [9] for the RBM mode Raman shift versus inner tube diameter expression. We observe a good agreement between the experimental and simulated patterns for the DWCNT-R sample. A somewhat less accurate agreement is observed for the DWCNT-N1, N2 samples, which may be related to the different growth method: arc discharge, as compared to laser ablation for the R and L samples. This agreement has important consequences for the understanding of the inner tube properties. As a result of the photoselective property of the Raman experiment, it proves that electronic structure of the inner tubes is identical in the different starting SWCNT materials. In addition, the diameter distribution of the inner tubes mimics that of the outer ones, a fact that has been speculated previously [8][11][19] and is established here. These properties of the inner tubes make them excellent probes of the diameter distribution of starting SWCNT materials, diameter selected SWCNTs and as shown in the following, motivates the study of diameter selective properties of the outer tubes.

In Fig. 2., we show the Raman spectra of the 60-DWCNT-N2 heat treated at 800 °C in dynamic vacuum for 40 minutes prior to the C_{60} encapsulation and DWCNT transformation as compared to an untreated sample. The spectra are normalized by the amplitude of the corresponding outer tubes. The weaker response at higher Raman shifted lines, i.e. inner tubes with smaller diameters is apparent in Fig. 2b. This is related to the annealing assisted closing of the outer tubes with small diameters, which prevents the C_{60} encapsulation. This effect is related to the higher reactivity for healing of openings in small diameter SWCNTs, which provide the host for the narrower inner tubes. Although, the overall healing effect and the more rapid closing of smaller nanotubes has been long anticipated, to our knowledge this is the first example when it is observed with an individual tube sensitivity. The technique allows the accurate determination of the healing speed of the different SWCNTs.

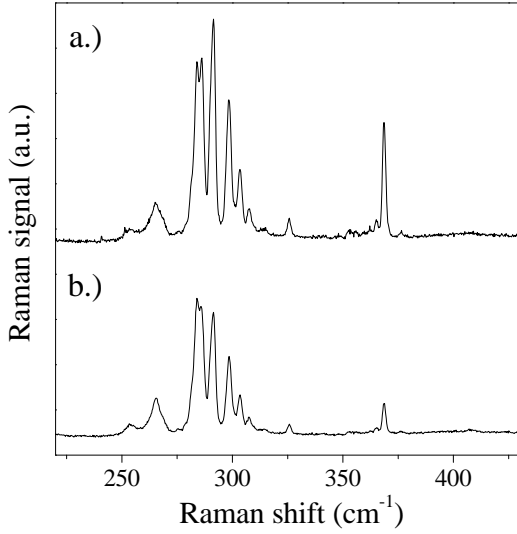


FIG. 2: Raman spectra of a.) untreated DWCNT-N2, b.) 800 °C prior to filling treated DWCNT-N2 sample at 647 nm excitation.

A systematic study will be published separately[20].

Fig. 3. compares the Raman spectra of 60- and 70-DWCNT-R for some representative laser energies. The RBMs of all the observable inner tubes, thus including the split components, can be found at the same position for all the 60-DWCNT and 70-DWCNT samples within our experimental precision. This reinforces the previous finding that the inner tube formation is robust against the starting SWCNT material or fullerene. The spectra shown in Fig. 3. are pair-wise normalized by the intensity of a selected inner tube from the 300-340 cm^{-1} spectral range. The photoselective property of the Raman experiments prevents the use of the same normalizing inner tube for all laser excitation energies. The observed similar pattern for 60-, 70-DWCNT proves that the electronic structure of the two kinds of DWCNT materials is identical.

The observation of the very small inner tubes, with Raman shifts ranging up to 430 cm^{-1} for 70-DWCNT is important. It was previously found [8] that the smallest observable inner tubes for 60-SWCNT are the (7,0), (5,3), (4,4) and (6,1) with diameters of 0.553, 0.553, 0.547, and 0.519 nm, respectively [9]. As indicated by solid arrows in Fig 3., we clearly observe the (7,0), (5,3) and (4,4) for the 70-DWCNT-R sample with intensities similar as in 60-DWCNT. The identification of the (6,1) tube is less certain as it appears with very small intensity already for the 60-DWCNT sample in the previous report [8]. Using the experimentally determined 0.72 nm inner and outer tube diameter difference[19], the cut-off of the inner tube distribution at the (6,1) tube for 60-DWCNT can be related to the smallest outer tube with $d_{\text{cut-off}, C_{60}} \approx 1.239$ nm where C_{60} can enter. This value is in reasonable agreement with theoretical estimates where $d_{\text{cut-off}, C_{60}} \approx 1.2$

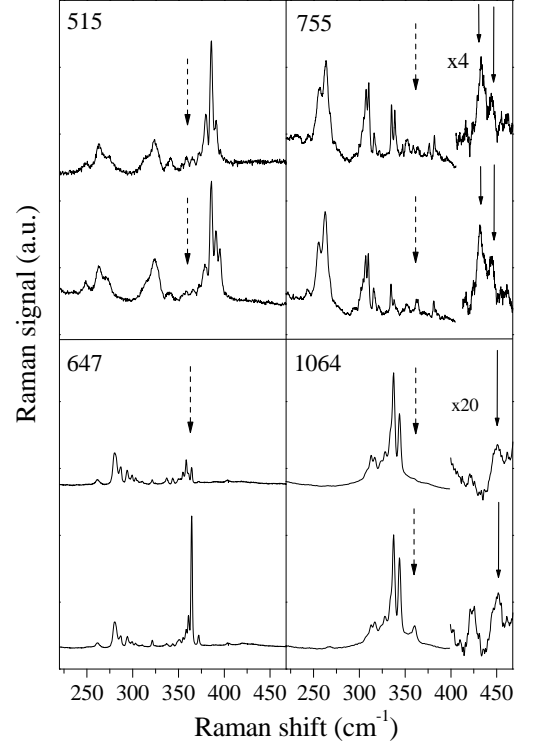


FIG. 3: Comparison of the Raman spectra of 60-DWCNT-R (lower spectra) and 70-DWCNT-R (upper spectra) for $\lambda=515$, 647, 755, and 1064 nm, respectively. Solid arrows indicate the (7,5) and (5,3) nanotubes in the 755 nm spectra and the (4,4) nanotube on the 1064 spectra. Dashed arrow mark the vicinity of the $362 \pm 3 \text{ cm}^{-1}$ spectral range.

nm was found for the smallest tube diameter where C_{60} peapod formation is energetically favored [21][22][23][24]. Similarly, the energetics of the C_{70} encapsulation was calculated and $d_{\text{critical}} \approx 1.35$ nm was found for the SWCNT diameter which separates the standing and lying configurations[25]. Based on this value, inner tubes with $d \lesssim 0.63$ nm can only be formed from C_{70} peapods in the lying configuration. The diameter of the above mentioned and arrow-indicated tubes in Fig. 3. are all well below this value. A small contamination of C_{60} of the C_{70} starting material can be excluded to explain for the observed smallest diameter inner tubes as it is unlikely to give rise to as many inner tubes as observed for the 60-DWCNT. Thus, it is evident that the smallest observed inner tubes for the 70-DWCNT are made nominally from lying C_{70} peapod molecules.

The above result has important implications on the theoretical models of the inner tube formation. It has been suggested that the route to inner tube growth is the formation of cyclo-additionally bonded precursor C_{60} dimers[12][13]. Once the dimers are formed, Stone-Wales transformations proceed till the completely formed inner tubes are developed. However, the lying C_{70} molecules are geometrically hindered to form cyclo-

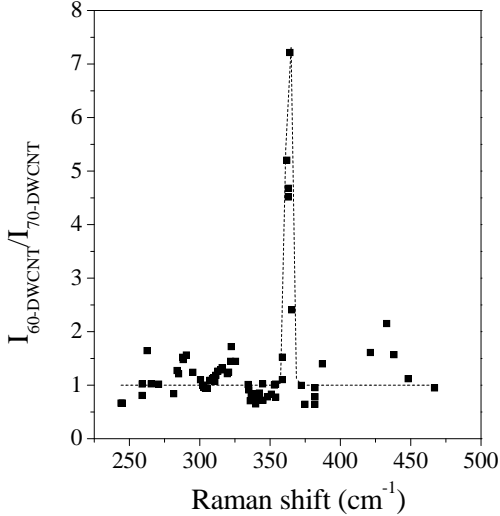


FIG. 4: Normalized intensity ratios of the Raman RBM modes of inner tubes in 60-, and 70-DWCNT-R materials at all laser lines studied. The data are sliding averaged as explained in the text. The dashed curve is guide to the eye.

additional dimers. Thus, the presence of inner tubes from lying C_{70} can not be explained by this model. Therefore, a different process must be anticipated for the formation of very small diameter inner tubes. If, however, an alternative mechanism is operational for inner tube growth from 'lying' C_{70} , it is reasonable to assume that the whole theory of inner tube formation requires revision. As an alternative possibility for the formation of inner tubes, a complete decay of the fullerenes into e.g. C_2 units may take place. This would be consistent with the observation that the particular geometry of the given fullerene does not play a role.

In what follows, an anomalous behavior observed for 70-DWCNTs with $d_{\text{outer}} \approx d_{\text{critical}}$ is discussed. The dashed arrows in Fig. 3. mark the vicinity of the $363 \pm 3 \text{ cm}^{-1}$ Raman shifted RBMs which were previously indentified to originate from the (5,5) metallic ($d = 0.68 \text{ nm}$) and the (8,1) semiconducting ($d = 0.671 \text{ nm}$) inner tubes along with their split components [8][9]. For a 647 nm excitation an unusual and unexpected behavior is observed. Within the Raman shift range indicated by the dashed arrows, some inner tube RBM components are significantly weaker for the 70-DWCNT samples as compared to the 60-DWCNT samples. This is consistent with the results of the 755 and 1064 nm excitations where weaker RBM modes are observed for the 70-DWCNT-R sample. We observed the same anomalous behavior for the 70-DWCNT samples prepared from the other SWCNT materials.

To quantify this effect, we compared the intensity ratio of the RBM modes of the inner tubes in 60-, and 70-DWCNTs for all the measured laser lines and for all

observed tubes. Voigtian lines were fitted to the observed spectra with a Gaussian width determined by the spectrometer response to the elastically scattered light (typically 1 cm^{-1}) and with a Lorentzian line-width of the corresponding RBM mode. As discussed above, we chose a particular tube in the $300\text{-}340 \text{ cm}^{-1}$ spectral range to normalize the observed inner tube RBM intensities before dividing the so-obtained values for the 60-, and 70-DWCNT by each other. Data points were collected together for the studied 8 laser energies and RBM modes, sorted by the RBM frequency and smoothed with a 3-point sliding averaging. This procedure reduces the noise of the intensity ratio and makes a data point more reliable when the same tube is observed at different laser energies. The result is summarized in Fig. 4. The anomaly of the intensity ratio is clearly observed in the $363 \pm 3 \text{ cm}^{-1}$ spectral range.

This spectral range corresponds to inner tubes with $d_{\text{inner}} \approx 0.67 \text{ nm}$ and $d_{\text{outer}} \approx 1.39 \text{ nm}$. As this latter value is close to the critical diameter separating the lying and standing C_{70} peapod configurations, it is tempting to associate the anomaly with the competition between the two configurations. This, $d_{\text{critical}} \approx 1.39 \text{ nm}$, value refines the theoretical result of $d_{\text{critical}} \approx 1.35 \text{ nm}$. We discuss two possible origins of the missing inner tubes: i) inability to form inner tubes from peapods filled with mixed lying and standing C_{70} configurations, ii) inability of C_{70} to enter into SWCNTs with $d_{\text{outer}} \approx d_{\text{critical}}$. It is possible that SWCNTs with $d_{\text{outer}} \approx d_{\text{critical}}$ are filled with mixed lying and standing C_{70} molecules. The previously proposed inner tube formation mechanism through dimer precursors followed by Stone-Wales transformations may explain the absence of inner tubes formed from such a mixture as the dimer formation might be very sensitive for the mutual alignment of two adjacent C_{70} molecules. However, we have shown that inner tubes are also formed from lying C_{70} molecules alone, which disfavors the idea that the precursor dimer is indeed necessary for the inner tube formation. Thus, it is speculated that the absence of inner tubes when $d_{\text{outer}} \approx d_{\text{critical}}$ is rather caused by the absence of C_{70} molecules for peapods with this diameter.

A mechanism involving impurities or side-wall defects can explain our observation: for the critical outer tube diameter separating the standing from the lying configuration one can expect that for a perfect tube the lying configuration is preferred. However, when side-wall defects or impurities are present, a C_{70} may change its configuration to a locally preferred standing one that may immobilize it thus preventing other C_{70} from entering into the tubes. Alternatively, a C_{70} molecule entering at the critical diameter may get trapped at a tube defect as e.g. a bend or kink and thus prevents further filling. In addition, the competition between elastic energy and rotation degrees of freedom may also give rise to a blocking of C_{70} in the tubes with $d_{\text{outer}} \approx d_{\text{critical}}$. The described diameter selective filling may provide a way to

mass-separate the unfilled peapod tubes from the filled ones. Interestingly, the outer tubes which remain unfilled are close to the well studied (10,10) tube.

In conclusion, DWCNT formation from peapods enables the study of diameter selective phenomena in SWCNT materials. The method provides a new and accurate tool for the characterization of directed nanotube growth, and the effects of subsequent treatments or diameter selective separation. The diameter selective closing of tube openings was observed for the first time. Comparison of C₆₀, C₇₀ peapod based DWCNT proves that the inner tube formation is a conservative process against the starting SWCNT or fullerene material. The presence of very small inner nanotubes in 70-DWCNT presents a challenge to the current theoretical models. The absence of mid-diameter inner tubes in 70-DWCNT is explained by the absence of C₇₀ peapods for the corresponding nanotube diameter due to the borderline between the lying and standing C₇₀ configurations.

This work was supported by the Austrian Science Funds (FWF) project Nr. 14893 and by the EU projects NANOTEMP BIN2-2001-00580 and PATONN Marie-Curie MEIF-CT-2003-501099 grants and by the Zoltan Magyary Fellowship. This study was partly supported by the Industrial Technology Research Grant Program in '03 from the New Energy and Industrial Technology Development Organization (NEDO) of Japan.

* Present address: Department of Applied & Environmental Chemistry, University of Szeged, Szeged, Hungary

- [2] M. S. Dresselhaus, G. Dresselhaus, P. C. Ecklund: *Science of Fullerenes and Carbon Nanotubes*, Academic Press, San Diego 1996.
- [3] D. Chattopadhyay *et al.*, J. Am. Chem. Soc. **125**, 3370 (2003).
- [4] R. Krupke *et al.*, Science **301**, 344 (2003).
- [5] Z. H. Chen *et al.*, Nano Lett. **3**, 1245 (2003).
- [6] M. Zheng *et al.*, Science **302**, 1545 (2003).
- [7] M. J. O'Connell *et al.*, Science **297**, 593 (2002).
- [8] R. Pfeiffer *et al.*, Phys. Rev. Lett. **90** 225501 (2003).
- [9] Ch. Kramberger *et al.*, Phys. Rev. B **68**, 235404 (2003).
- [10] B. W. Smith, M. Monthieux, and D. E. Luzzi, Nature (London) **396** 323 (1998).
- [11] S. Bandow *et al.*, Chem. Phys. Lett. **337** 48 (2001).
- [12] D. Tománek, private communication.
- [13] Y. Zhao, B. I. Yakobson, R. E. Smalley, Phys. Rev. Lett. **88**, 185501 (2002).
- [14] K. Hirahara *et al.*, Phys. Rev. B. **64**, 115420 (2001).
- [15] H. Kataura *et al.*, Appl. Phys. A **74**, 349 (2002).
- [16] <http://www.nanocarblab.com>
- [17] H. Kataura *et al.*, Synth. Met. **121**, 1195 (2001).
- [18] H. Kuzmany *et al.*, Eur. Phys. J. B **22**, (2001) 307.
- [19] M. Abe *et al.*, Phys. Rev. B **68**, (2003) 041405.
- [20] F. Hasi *et al.*, unpublished.
- [21] M. Melle-Franco *et al.*, J. Phys. Chem. B, **109**, 6986 (2003).
- [22] S. Berber, Y-K. Kwon, D. Tománek, Phys. Rev. Lett. **88**, 185502 (2002).
- [23] A. Rochefort, cond-mat/0301310.
- [24] M. Otani, S. Okada, and A. Oshiyama, Phys. Rev. B **68**, 125424 (2003).
- [25] S. Okada, M. Otani, and A. Oshiyama, New J. Phys. **5**, 122 (2003).